Eur. Phys. J. A **25**, s01, 315–320 (2005)
DOI: 10.1140/epjad/i2005-06-080-6

EPJ A direct
electronic only

New insights into the resonance states of ^{5}H and ^{5}He

G.M. Ter-Akopian[1,a], A.S. Fomichev[1], M.S. Golovkov[1], L.V. Grigorenko[1], S.A. Krupko[1], Yu.Ts. Oganessian[1], A.M. Rodin, S.I. Sidorchuk[1], R.S. Slepnev[1], S.V. Stepantsov[1], R. Wolski[1,2], A.A. Korsheninnikov[3,b], E.Yu. Nikolskii[3,b], P. Roussel-Chomaz[4], W. Mittig[4], R. Palit[5], V. Bouchat[6], V. Kinnard[6], T. Materna[6], F. Hanappe[6], O. Dorvaux[7], L. Stuttge[7], C. Angulo[8], V. Lapoux[9], R. Raabe[9], L. Nalpas[9], A.A. Yukhimchuk[10], V.V. Perevozchikov[10], Yu.I. Vinogradov[10], S.K. Grishechkin[10], and S.V. Zlatoustovskiy[10]

[1] Joint Institute for Nuclear Research, Dubna, 141980 Russia
[2] The Henryk Nievodniczański Institute of Nuclear Research, Cracow, Poland
[3] RIKEN, 2-1 Hirosawa, Wako, Saitama 351-0198, Japan
[4] GANIL, BP 5027, F-14076 Caen Cedex 5, France
[5] Gesellschaft für Schwerionenforschung, D-64231 Darmstadt, Germany
[6] Université Libre de Bruxelles, PNTPM, Brussels, Belgium
[7] Institut de Recherches Subatomique, IN2P3/Université Louis Pasteur, Strasbourg, France
[8] Centre de Recherche du Cyclotron, UCL, Chemin du Cyclotron 2, B-1348 Louvain-La-Neuve, Belgium
[9] DSM/DAPNIA/SPhN, CEA Saclay, F-91191 Gif-sur-Yvette Cedex, France
[10] RNFC – All-Russian Research Institute of Experimental Physics, Sarov, Nizhni Novgorod Region, 607190 Russia

Received: 10 December 2004 / Revised version: 18 February 2005 /
Published online: 27 May 2005 –

Abstract. The ^{5}H system was produced in the ^{3}H$(t,p)^5$H reaction studied at small CM angles with a 58 MeV tritium ion beam. High statistics data were used to reconstruct the energy and angular correlations between the ^{5}H decay fragments. A broad structure in the ^{5}H missing-mass spectrum showing up above 2.5 MeV was identified as a mixture of the $3/2^+$ and $5/2^+$ states. The data also present an evidence that the $1/2^+$ ground state of ^{5}H is located at about 2 MeV. Then, the ^{5}H and ^{5}He systems were explored by means of transfer reactions occurring in the interactions of 132 MeV ^{6}He beam nuclei with deuterium. In the ^{2}H(^{6}He,^{3}H) reaction a $T = 3/2$ isobaric analog state of ^{5}H in ^{5}He was observed at an excitation energy of 22.0 ± 0.3 MeV with a width of 2.5 ± 0.3 MeV.

PACS. 25.10.+s Nuclear reactions involving few-nucleon systems – 25.60.-t Reactions induced by unstable nuclei – 25.60.Je Transfer reactions – 27.10.+h Properties of specific nuclei listed by mass ranges: $A \leq 5$

1 Introduction

A number of experimental papers [1,2,3,4,5] published recently presented rather contradictory data about the position and width of the $J^\pi = 1/2^+$ ground state (g.s.) resonance of the ^{5}H nuclear system. Controversy in results obtained to date on the ^{5}H system caused intense discussions (see a review in ref. [6]). Essentially, the question is whether the ^{5}H g.s. is located at 1.7–1.8 MeV above the $t + 2n$ decay threshold [3,4], or at about 3 MeV [5] or even higher [1,2]. Consequently, new experiments must be carried out if this question is to be resolved. This is important also for planning future experiments aimed at the even heavier hydrogen nucleus ^{7}H [7].

We report here on a new study made for the ^{5}H system obtained in the same ^{3}H$(t,p)^5$H reaction as in ref. [4][1]. We also explored the ^{2}H(^{6}He,^{3}He)^{5}H and ^{2}H(^{6}He,^{3}H)^{5}He reactions to observe the g.s. in ^{5}H and the lowest $T = 3/2$ state in ^{5}He. These two reactions correspond to the transfer of either proton or neutron from the α core of ^{6}He to the deuterium target nucleus. The kinematics of these reactions is similar, and their relative yields are governed by the isospin selection rule.

2 Experimental conditions

We studied the ^{3}H$(t,p)^5$H reaction using a 58 MeV beam of tritium ions accelerated by the U-400M (JINR, Dubna) cyclotron. The ACCULINNA separator [9] was used to

[a] e-mail: Gurgen.TerAkopian@jinr.ru
[b] On leave from the Kurchatov Institute, Kurchatov sq. 1, Moscow, 123182 Russia.

[1] Since the time of the ENAM conference this material has been partly published in ref. [8].

reduce the angular spread and energy dispersion of the primary triton beam to 7 mrad and 0.3 MeV (FWHM), respectively. Finally, the triton beam with intensity of $3 \cdot 10^7\,s^{-1}$ was focused in a 5 mm spot on a cryogenic tritium target [10]. The 4 mm thick target cell, having twofold 6 μm stainless steel windows on each side, was filled with tritium to a pressure of 860 mbar and cooled down to 25 K. The thickness of the tritium target was 2.2×10^{20} atoms/cm^2. The missing-mass energy spectrum of ^{5}H was derived from the energies and emission angles measured by means of an annular Si detector for the protons emitted to the backward direction. The measurements covered center-of-mass (CM) angles between 3.5° and 10.0°. Due to the kinematic focusing, the ^{5}H decay products $(t + 2n)$ were detected in wide ranges of their emission angles. Tritons moving in the forward direction in laboratory system were detected by a telescope consisting of four annular Si detectors. Neutrons were detected by 48 scintillation modules of the time-of-flight neutron spectrometer DEMON [11].

Secondary ^{6}He beam from the ACCULINNA separator was used to study the reactions ^{2}H(^{6}He,^{3}He)^{5}H and ^{2}H(^{6}He,^{3}H)^{5}He. The beam intensity and energy were, respectively, 3×10^5 pps and 132 MeV. Angular and position resolutions of $\pm 0.2°$ and 1.25 mm were achieved by tracking individual ^{6}He ions hitting the deuterium target. The kinetic energy of each ^{6}He was measured with accuracy 1.6% by means of a pair of time-of-flight detectors. The target cell was filled at 1 atm with a high purity deuterium gas and cooled down to 25 K. It had 6 μm stainless steel entrance and exit windows. The thickness of the deuterium target was 2.6×10^{20} atoms/cm^2. The missing-mass energy spectra of ^{5}H and ^{5}He nuclei were derived, respectively, from the energies and emission angles measured for the ^{3}He and ^{3}H nuclei formed in the reactions ^{2}H(^{6}He,^{3}He)^{5}H and ^{2}H(^{6}He,^{3}H)^{5}He. The first, trigger telescope detected relatively low energy ^{3}He and ^{3}H nuclei emitted at laboratory angles $\theta_{\mathrm{lab}} = 25° \pm 7°$. In coincidence with these low energy ^{3}He and ^{3}H nuclei we detected charged particles emitted as the decay products of ^{5}H and ^{5}He. The second, slave telescope was used to detect these high energy ^{3}H nuclei originating from the $t+2n$ decay of ^{5}H and high energy charged particles from different decay modes possible for the ^{5}He nucleus: $^5\mathrm{He} \to {}^3\mathrm{He} + n + n$, $^5\mathrm{He} \to d + p + n$, $^5\mathrm{He} \to \alpha + n$, $^5\mathrm{He} \to t + d$. The measurements made for such coincidence events covered a CM angular range of 21°–40° for each of these reactions: ^{2}H(^{6}He,^{3}He)^{5}H and ^{2}H(^{6}He,^{3}H)^{5}He. Due to the difference in the energy of the reaction ejectiles and the decay products of ^{5}H and ^{5}He, the corresponding kinematical branches of these reactions were uniquely identified.

3 Results and discussion

3.1 Study of the ^{3}H$(t, p)^5$H reaction

In the case of the ^{3}H$(t,p)^5$H reaction we discuss only the *ptn* coincidence data. Such coincidence events uniquely identify the $p + {}^5$H outgoing channel and make possible a complete kinematic reconstruction. The ^{5}H missing-mass spectrum measured with a 0.4 MeV resolution in energy is presented in fig. 1. We measured this spectrum up to 5 MeV. The 5.5 MeV limit is caused by the detection threshold for slow protons moving in the backward direction. The smooth, continuum nature of this high statistics spectrum do not leave any chance for a narrow resonance state which one could attribute to ^{5}H. However, much more informative are correlations revealed for the decay products of this nucleus. Figure 2 shows the distribution of the ^{5}H decay energy ($E_{^5\mathrm{H}}$) between the relative motions in the t-nn and nn subsystems (presented in terms of the $E_{nn}/E_{^5\mathrm{H}}$ ratio). It shows a narrow peak corresponding to a strong n-n final-state interaction (FSI). The most

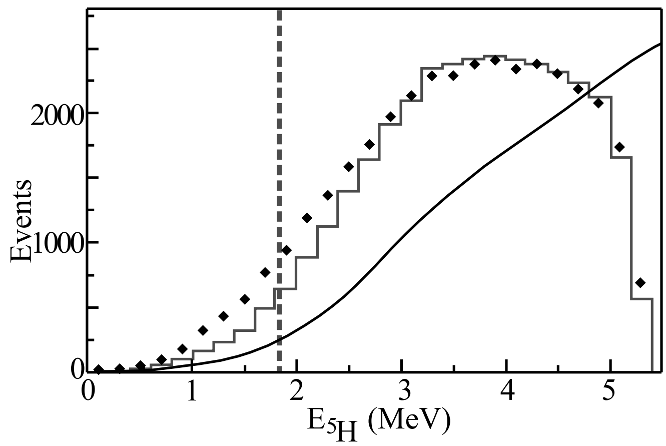

Fig. 1. Missing-mass spectrum of ^{5}H. Diamonds show the experimental data points. The vertical dashed line shows the position of the ^{5}H g.s. deduced in refs. [3,4]. The histogram is the result of Monte Carlo (MC) simulation and the solid curve is the input for MC simulation. Here and below, the data points show the real numbers of detected events. The statistical errors are not shown.

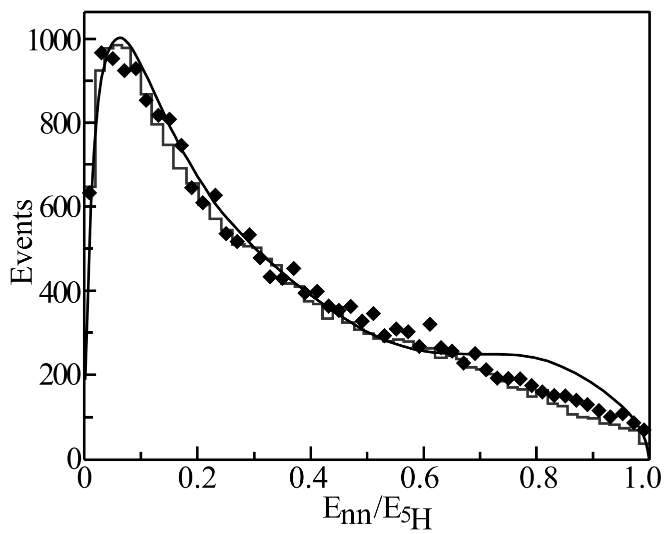

Fig. 2. Relative energy spectrum for two neutrons. The plot details are the same as in in fig. 1.

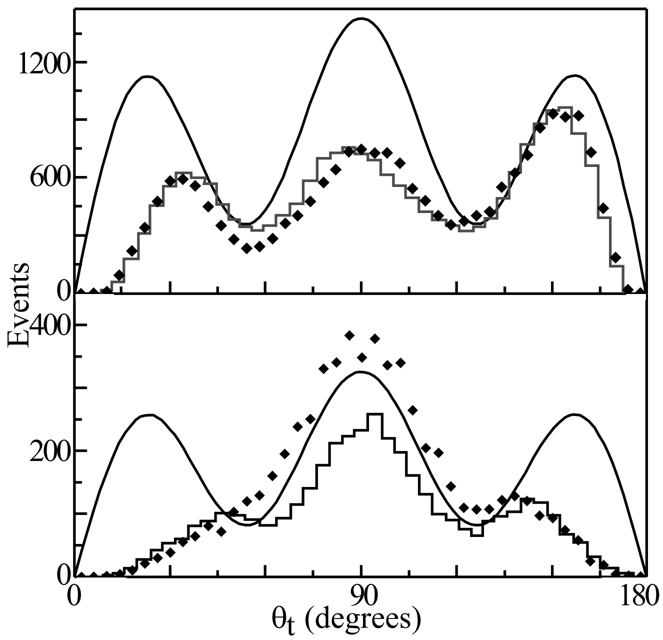

Fig. 3. Angular distributions of tritons in the ^{5}H frame for the two ranges of the ^{5}H energy: 3.5–5.5 MeV (upper panel) and 0–2.5 MeV (lower panel). θ_t is the triton emission angle taken in respect to Z-axis chosen to coincide with the direction of the momentum transfer $\mathbf{k}_{\rm beam} - \mathbf{k}_p$ occurring in the reaction ^{3}H$(t,p)^5$H. The plot details here are the same as in fig. 1.

striking result is the observation of a sharp oscillating picture in the triton angular distribution shown in fig. 3.

Such a sharp oscillating angular distribution can be obtained only for very specific conditions. To our knowledge, only one observation of oscillating pattern was reported for the reaction involving nuclei with non-zero spin: ^{13}C$(^6$Li$,d)^{17}$O$^*(\alpha)^{13}$C$_{\rm g.s.}$ [12]. It was shown in ref. [13] that the energy degeneracy and interference of (at least) two states are required to reproduce the observed correlations.

Calculations were made with assumption that a single J^π state (either $3/2^+$ or $5/2^+$) is populated in the ^{5}H system formed in the reaction ^{3}H$(t,p)^5$H. These calculations made us sure that the strongly oscillating distribution shown in fig. 3 can not be obtained for ^{5}H assuming the population of one selected J^π state. At the same time it appeared that the bulk of data observed in the present experiment can be explained by the assumption that the direct transfer of two neutrons ($\Delta L = 2$, $\Delta S = 0$) dominates in the ^{3}H$(t,p)^5$H reaction leading to the population of the broad, overlapping $3/2^+$ and $5/2^+$ states. The idea is supported by the following arguments.

The ^{5}H system could be considered as a "proton hole" in ^{6}He (*e.g.*, [14]), so definite similarities can be expected between these systems. Theoretical predictions give $J^\pi = 1/2^+$ for the g.s. of ^{5}H. The low lying excited states are supposed to be a $3/2^+$ and $5/2^+$ doublet. One should expect a weak population of the ^{5}H g.s. in the ^{3}H$(t,p)^5$H reaction due to the statistical factor and also as a consequence of the "angular momentum mismatch" that arises from the fact that the light proton can not carry away as much angular momentum as the heavier triton projectile brings in. DWBA calculations confirm this idea indicating that the momentum transfers $\Delta L = 1$, 2 dominate, whereas $\Delta L = 0$ is suppressed by about one order of magnitude even at forward angles. The spin transfer is negligible in this reaction. $\Delta S = 1$ is possible only if the two neutrons are in a negative parity state of relative motion. The previous experience shows that this is highly improbable in contrast to the "dineutron" transfer, which is known to be a good approximation valid in a broad range of transfer reactions. The $3/2^+$ and $5/2^+$ states can be considered as degenerate. Theory calculations (*e.g.*, [14]) show that the expected energy split between these states is much less than their widths. To produce the strongly oscillating picture, the domination of the $\{L = 2, S_x = 0, l_x = 0, l_y = 2\}$ component in the structure of the ^{5}H wave function is necessary (L is the total angular momentum, subscripts x and y refer to the spins and angular momenta of nn and t-nn subsystems). This is a reasonable expectation supported both by the analysis of experimental data [15] and theoretical calculations [16] made for the ^{6}He 2^+ state.

We employed the following procedure for data analysis. Correlations occurring at the ^{5}H decay are described as

$$W = \sum_{JM,J'M'} \langle J'M'|\rho|JM\rangle \; A^\dagger_{J'M'} A_{JM} \, ,$$

where J, M are the total ^{5}H spin and its projection, A_{JM} are the decay amplitudes depending on the ^{5}H decay dynamics. $\langle J'M'|\rho|JM\rangle$ is the density matrix, which describes the polarization of the ^{5}H states populated in the ^{3}H(t,p) reaction and takes into account the mixing of the $3/2^+$ and $5/2^+$ states. It was parameterized assuming azimuthal symmetry with respect to the momentum transfer in the ^{3}H(t,p) reaction. This assumption is well confirmed by the experimental data and reduces to 5 the number of independent parameters. All elements of the density matrix were assumed to have the same energy dependence and were represented by splines. The amplitudes A_{JM} were expanded over a limited set of hyperspherical harmonics (assumed to be the same for the $3/2^+$ and $5/2^+$ states). A similar approach has been used in ref. [17], where the non-isotropic three-particle decay of ^{6}Be(2^+) state has been explored. The hyperspherical expansions of the decay amplitudes were also used for the analysis of $A = 6$ [15,18] and ^{5}H [5,6] decay data.

Parameters of the ρ-matrix and hyperspherical expansion were treated as free in our analysis. A complete MC simulation of the experiment has been performed. In this way, analytical expressions were extracted for the decay probability in the multidimensional space, corrected for the setup efficiency. Projections of the extracted distributions (solid curves) and the results of MC simulations (histograms) are shown in figs. 1-3. The amplitudes and relative arguments obtained for the hyperspherical components are listed in table 1.

Agreement obtained between the experimental data and the MC results is excellent at $E_{^5\rm H} > 2.5$ MeV (see

Table 1. Hyperspherical decompositions of decay amplitudes A_{JM} for the excited states of ^{5}H ($E_{^5\mathrm{H}} = 2.5$–$5.5\,\mathrm{MeV}$) (the squared moduli of the partial amplitudes are given in percents and relative arguments in degrees). The errors given for our fit are pure statistical; the other uncertainties discussed in ref. [15] are valid also for the present analysis.

K	L	l_x	l_y	S_x	mod^2	arg
2	2	0	2	0	35 ± 2	0
4	2	0	2	0	37 ± 2	58 ± 1
6	2	0	2	0	8.0 ± 1.5	138 ± 6
2	2	2	0	0	20 ± 2	180 ± 3
2	1,2	1	1	1	<3	

upper panel in fig. 3). Below this energy, we could not achieve an agreement assuming the interference of only $3/2^+$ and $5/2^+$ states. This can be well seen in fig. 3 (lower panel). The impact of this disagreement on the ^{5}H missing-mass spectrum is also seen in fig. 1 in the deviation of the MC results from the experimental data below 3 MeV. We can reproduce the correlations obtained at $E_{^5\mathrm{H}} < 2.5\,\mathrm{MeV}$ by assuming the interference of the $1/2^+$ g.s. with the $3/2^+$–$5/2^+$ doublet. One can take this as an evidence for the population of the ^{5}H g.s. lying at about 2 MeV.

Interference of the $1/2^+$, $3/2^+$, and $5/2^+$ states becomes possible in the ^{5}H missing-mass spectrum when the detection probability of the ^{5}H decay fragments depends on their emission angles. This dependence was strongly pronounced in ref. [4] and had a place in this work. Interference was considered in ref. [4] as a possible explanation for the too small width of the ^{5}H peak observed at 1.8 MeV. The interference of the ^{5}H g.s. with the $3/2^+$–$5/2^+$ doublet, apparently showing up in the correlation patterns observed in the present work at $E_{^5\mathrm{H}} < 2.5\,\mathrm{MeV}$, supports this assumption of ref. [4].

Good quality description of data presented in fig. 2 and, especially, in fig. 3 supports the assumption that the ^{5}H states are populated in the reaction utilized in this study. A combination of direct processes with a pairwise FSI can hardly give such a result.

3.2 Resonance states of ^{5}H and ^{5}He in ^{6}He + ^{2}H collisions

To identify the ^{2}H(^{6}He,^{3}He)^{5}H reaction we analyzed such events where relatively low energy ^{3}He nuclei ($T_{\mathrm{lab}} \leq 20\,\mathrm{MeV}$) were detected by the the trigger telescope in coincidence with tritons which were the ^{5}H decay products. The tritons were detected by the slave telescope. The obtained ^{5}H missing-mass energy spectrum is shown in fig. 4.

Reaction ^{2}H(^{6}He,^{3}H)^{5}He became apparent when low energy tritons ($T_{\mathrm{lab}} \leq 20\,\mathrm{MeV}$) were detected by the trigger telescope in coincidence with charged particles originating from the ^{5}He decay. First of all we were interested in the ^{5}He decay modes which were expected for the $T = 3/2$ isobaric analog state. In order to satisfy the isospin selection rule, pure $T = 3/2$ states in ^{5}He must decay by the emission of three particles, $^3\mathrm{He}+n+n$ and $t + p + n$. For $T = 1/2$ states, there are the well known two-particle decays $t + d$ and $\alpha + n$. Thus, to build missing-mass energy spectra for ^{5}He nuclei formed in resonance states with isospin $T = 3/2$, we used events where the low energy tritons were detected in coincidence with ^{3}He, tritons or protons (we refer to these events as to the t-^{3}He, t-t and t-p coincidences). Due to the precise measurements made for the energies and trajectories of coincident particles we could separate the t-t coincidences originating from the $^5\mathrm{He} \to t+p+n$ decays from those t-t coincidence events which appeared due to the two-particle decay $^5\mathrm{He} \to t + d$. The two spectra presented in fig. 5 were built for the tree-particle decay modes of ^{5}He using the t-^{3}He coincidences (upper panel) and the sum of the t-t and t-p coincidences (lower panel).

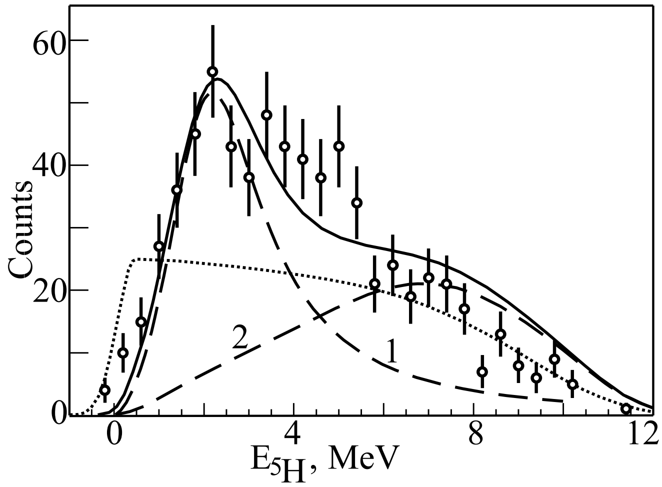

Fig. 4. Missing-mass energy spectrum of ^{5}H from the ^{2}H(^{6}He,^{3}He) reaction. The ^{5}H energy is presented relative to the $t+n+n$ decay threshold. Curve 1 is the three-body decay curve with resonance energy $E_{\mathrm{res}} = 2.2 \pm 0.3\,\mathrm{MeV}$ and width $\Gamma^{\mathrm{obs}} \simeq 2.5\,\mathrm{MeV}$ (see text). Curve 2 shows the phase space spectrum with the $n+n$ FSI. The solid curve is the sum of curve 1, folded with the resolution and weighted with the efficiency, and the phase space curve 2. The dotted curve shows the detection efficiency folded with the resolution (arbitrary units).

Steep ascents setting in just near the decay thresholds and the overall similarity of the spectra shown in figs. 4, 5 are clear indications that we see similar nuclear resonance states in the systems with mass number $A = 5$ which decay into three particles. To describe these resonance states, showing the three-body decays, we used analytical expression obtained in ref. [19]. The spectra in figs. 4, 5 were fitted as sums of the resonance state and the three-body phase space spectra for $t+n+n$, $^3\mathrm{He}+n+n$ and $t+p+n$ with the $n + n$ and $n + p$ FSI.

Data in fig. 4 can be described within two standard deviations assuming a single resonance with energy varied between 1.8 and 2.6 MeV and width $\Gamma^{\mathrm{obs}} \simeq 2.5\,\mathrm{MeV}$, alongside with the phase space. One can not more precisely estimate the ^{5}H g.s. resonance parameters as the acquired statistics prevents one from any accurate separation from the excited states of this nucleus presumably

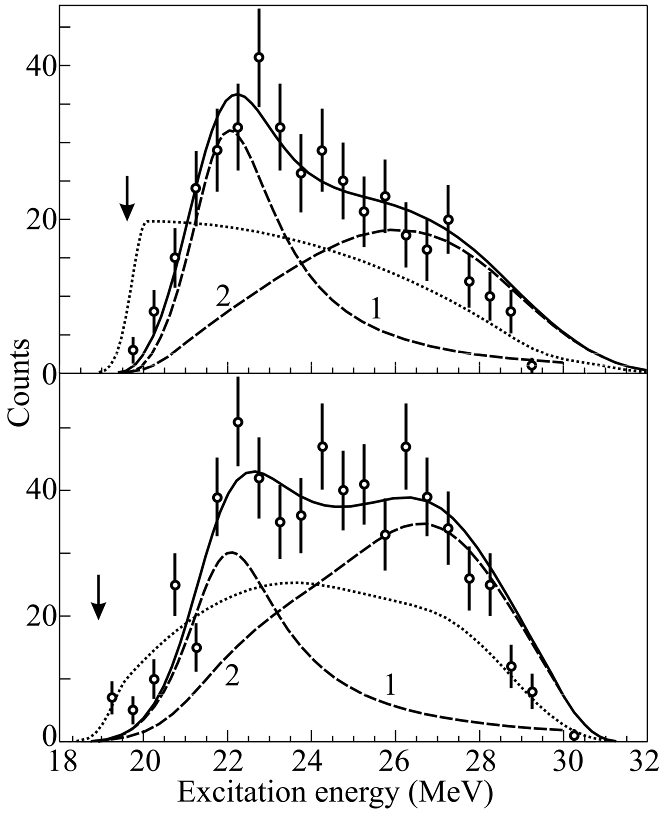

Fig. 5. Missing-mass excitation energy spectrum of ^{5}He from the ^{2}H(^{6}He, t) reaction. The excitation energy is presented relative to the ^{5}He g.s. resonance energy. The upper panel shows the spectrum obtained for t+^{3}He coincidences. The lower panel shows the spectrum obtained for the t+t and t+p coincidences. The vertical arrows indicate the $^5\mathrm{He} \to {}^3\mathrm{He} + n + n$ (upper panel) and the the $^5\mathrm{He} \to t+p+n$ (lower panel) decay thresholds. Curve 2 in upper and lower panels show the corresponding phase space spectra with $n+n$ (upper panel) and $n+p$ (lower panel) FSI. Other notations are as in fig. 4.

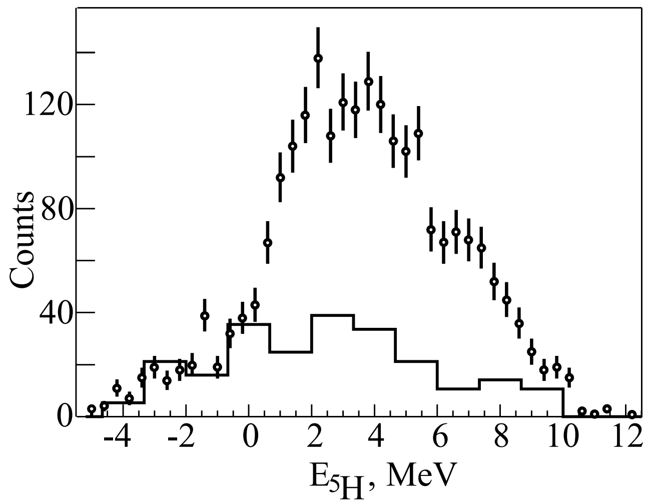

Fig. 6. Missing-mass energy spectrum of ^{5}H, relative to the $t+n+n$ decay threshold, derived from inclusive data obtained for ^{3}He ejectiles detected in the trigger telescope from the ^{2}H(^{6}He,^{3}He) reaction. The background obtained with the empty target cell is shown by the solid line histogram.

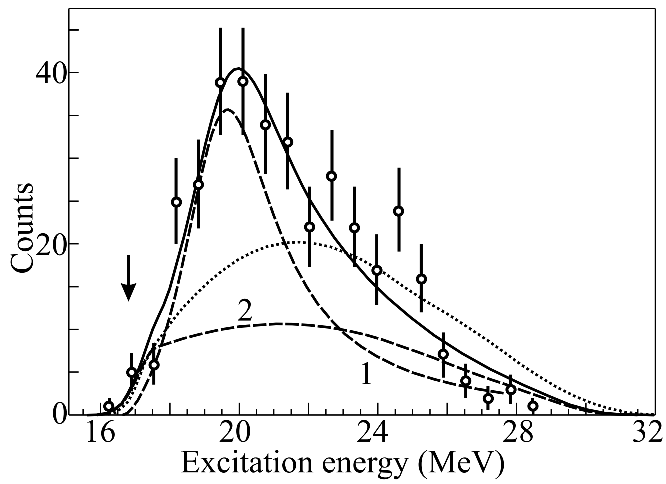

Fig. 7. Missing-mass excitation energy spectrum of ^{5}He from the ^{2}H(^{6}He,^{3}H) reaction, obtained for $t+d$ coincidences. The vertical arrow shows the $^5\mathrm{He} \to t$+d threshold. Other notations are as in fig. 4.

populated in the same reaction. Taking this consideration into account, we are inclined rather to say that the ^{5}H g.s. resonance energy and width inferred from fig. 4 do not contradict results presented in ref. [3]. In favor of this says also the ^{5}H spectrum derived from the inclusive ^{3}H ejectile data (see fig. 6). This agrees also with the ^{5}H g.s. resonance position presented in ref. [4].

From the fit shown in fig. 4 we estimated a value of about 0.3 mb/sr for the cross-section of the reaction ^{2}H(^{6}He,^{3}He)^{5}H populating the g.s. resonance in ^{5}H. The error of this value may amount to as much as 50% in magnitude because of the uncertainty from the contribution of the ^{5}H excited states.

Data presented in fig. 5 indicate that we have observed a ^{5}He resonance state with isospin $T = 3/2$, located at an excitation energy $E^{\mathrm{obs}} = 22.0 \pm 0.3\,\mathrm{MeV}$ and having a width $\Gamma^{\mathrm{obs}} = 2.5 \pm 0.3\,\mathrm{MeV}$. We found that this state showed up in the ^{5}He three-body decay modes allowed for the $T = 3/2$ state. The cross-sections were estimated to be, respectively, 0.10 ± 0.03 mb/sr and 0.2 ± 0.1 mb/sr for the $^5\mathrm{He} \to {}^3\mathrm{He} + n + n$ and $^5\mathrm{He} \to t + p + n$ decay modes of the isobaric analog state. For this 22.0 MeV ^{5}He state we did not observe the $t + d$ decay mode which is allowed only for a $T = 1/2$ state.

However, we could measure the $t + d$ decay of the $T = 1/2$, $J^\pi = 3/2^-$ resonance state of ^{5}He located at about 20 MeV, according to ref. [20]. Figure 7 shows the missing-mass energy spectrum of ^{5}He derived from the $t + d$ coincidence events associated with the $t + d$ decay of ^{5}He nuclei produced in the ^{2}H(^{6}He,^{3}H) reaction. In fact, in the ^{5}He excitation energy region extending from 19 to 20 MeV there are four broad $T = 1/2$ states of ^{5}He with $J^\pi = 5/2^+$, $3/2^+$, $7/2^+$ and $3/2^-$ derived in [20] in the framework of the extended R-matrix theory. The $3/2^-$ state ought to be the most probably populated via the ^{2}H(^{6}He,^{3}H) reaction. Fitting the spectrum in fig. 7 with a single-level Breit-Wigner formula we found that this $J^\pi = 3/2^-$ state of ^{5}He was located at $E_{\rm res} = 19.7 \pm 0.3$ MeV (curve 1 in fig. 7). This fit corresponds to a cross-section of 0.3 ± 0.1 mb/sr. The contribution from the energetically allowed three-body decays of this $T = 1/2$ state in the region of the 22.0 MeV isobaric analog $T = 3/2$ state was estimated to be less than 10%.

We did not see the $t + d$ decay mode of the well known 16.8 MeV ($J^\pi = 3/2^+$) state of ^{5}He as our detection efficiency was too low for this excitation energy (see the detection efficiency curve shown in fig. 7). We also could not see the $\alpha + n$ decay mode of this ^{5}H resonance state as well as the $\alpha + n$ decay mode of the observed 19.7 MeV resonance. This is well explained as due to the high background from the reaction ^{2}H(^{6}He,α) resulting in the formation of the ^{4}H nucleus in its ground state.

4 Conclusions

Missing-mass spectrum obtained in the ^{3}H$(t,p)^5$H reaction shows a broad structure above 2.5 MeV. The observed strong correlation pattern allows us to unambiguously identify this structure as a mixture of the $3/2^+$ and $5/2^+$ states in ^{5}H. Such correlation is a rare phenomenon for transfer reactions involving particles with nonzero spin and means that the $3/2^+$ and $5/2^+$ states are either almost degenerate or the reaction mechanism causes a very specific interference of these states.

Excited states observed in this ^{5}H energy range support the conclusion made in ref. [3] about the ^{5}H g.s. resonance position at 1.7 ± 0.3 MeV. The correlation picture obtained at $E_{^5\rm H} < 2.5$ MeV (see fig. 3) gives evidence for the interference of the $3/2^+$–$5/2^+$ doublet with the $J^\pi = 1/2^+$ g.s. in ^{5}H. This is consistent with the alternative explanation presented in ref. [4] for the small width of the observed 1.8 MeV g.s. peak of ^{5}H. Indeed, the interference can cause such a distortion of the ^{5}H g.s. resonance inherently having a sizeable width.

Analysis made for angular and internal energy correlations in ^{5}H shows a reasonable agreement between the structure deduced for ^{5}H and the structure calculated or deduced from experimental data in the case of ^{6}He 2^+ state (see refs. [15,18]).

By studying the three-body decay modes $^5\text{He} \to {}^3\text{He} + n + n$ and $^5\text{He} \to t + p + n$ we have identified for the first time the isobaric analog of the ^{5}H g.s. resonance in ^{5}He formed in the ^{2}H(^{6}He,^{3}H)^{5}He reaction. We have made sure that the 19.7 MeV ($J^\pi = 3/2^-$, $T = 1/2$) resonance state known for ^{5}He does not show these three body decay modes. The $T = 3/2$ isobaric analog state is located at a ^{5}He excitation energy of 22.0 ± 0.3 MeV and has a width of 2.5 ± 0.3 MeV.

Simultaneously, we observed the g.s. resonance of ^{5}H populated in the reaction ^{2}H(^{6}He,^{3}He) Data obtained for this reaction allowed us to come to a conclusion that the ^{5}H g.s. resonance is located at about 2 MeV above the $^5\text{H} \to t + n + n$ decay threshold. This does not contradict the data on the energy of the ^{5}H g.s. resonance presented in refs. [3,4].

Assuming the isospin invariance of nuclear forces the excitation energy of the isobaric analog state in ^{5}He can be estimated from the neutron-proton mass difference and Coulomb energy $0.6Z(Z-1)/A^{1/3}$ [20]. For a ^{5}H g.s. at ~ 2 MeV, the $T = 3/2$ analog state should exist in ^{5}He at an excitation energy of ~ 21.7 MeV. Taking into consideration experimental errors assigned to the energy positions of the resonance states, we conclude that the energies observed for the ^{5}H g.s. resonance and its isobaric analog in ^{5}He are in mutual accord.

Our data show that the cross-sections of the $1p/1n$-transfers from the α core of the ^{6}He nucleus to deuteron resulting in the formation of the $T = 3/2$ states of ^{5}H/^{5}He are close to each other in their values. In the strict sense of the isospin selection rule, the cross-section ratio of the two reactions leading to the ^{5}H g.s. and to the lowest $T = 3/2$ state in ^{5}He should equal 3. However, isospin mixing and/or reaction dynamics could be a plausible reason of the approximate equality obtained for these cross-sections.

As a whole, the observation of the $T = 3/2$ isobaric analog state in ^{5}He with the energy and width given above presents an additional argument in favor of the conclusions drawn in refs. [3,4] about the ^{5}H g.s. resonance.

Partial support of the work by the Russian Basic Research Foundation (grant No. 02-02-16550) and by the INTAS grant No. 03-51-4496 is acknowledged.

References

1. D.V. Aleksandrov *et al.*, *Proceedings of the International Conference on Exotic Nuclei and Atomic Masses, (ENAM95), Arles, France, 1995* (Editions Frontiers, Gif-sur-Yvette, France, 1995) p. 329.
2. M.G. Gornov *et al.*, JETP Lett. **77**, 344 (2003).
3. A.A. Korsheninnikov *et al.*, Phys. Rev. Lett. **87**, 092501 (2001).
4. M.S. Golovkov *et al.*, Phys. Lett. B **566**, 70 (2003).
5. M. Meister *et al.*, Phys. Rev. Lett. **91**, 162504 (2003).
6. L.V. Grigorenko, Eur. Phys. J. A **20**, 419 (2004).
7. M.S. Golovkov *et al.*, Phys. Lett. B **588**, 163 (2004).
8. M.S. Golovkov *et al.*, Phys. Rev. Lett. **93**, 262501 (2004).
9. A.M. Rodin *et al.*, Nucl. Instrum. Methods B **126**, 236 (1997).
10. A.A. Yukhimchuk *et al.*, Nucl. Instrum. Methods A **513**, 439 (2003).
11. I. Tilquin *et al.*, Nucl. Instrum. Methods A **365**, 446 (1995).
12. K.P. Artemov *et al.*, Yad. Fiz. **28**, 288 (1978).
13. G. Cardella *et al.*, Phys. Rev. C **36**, 2403 (1987).
14. N.B. Shul'gina *et al.*, Phys. Rev. C **62**, 014312 (2000).
15. B.V. Danilin *et al.*, Sov. J. Nucl. Phys. **46**, 225 (1987).
16. B.V. Danilin *et al.*, Nucl. Phys. A **632**, 383 (1998).
17. O.V. Bochkarev *et al.*, Sov. J. Nucl. Phys. **55**, 955 (1992).
18. O.V. Bochkarev *et al.*, Nucl. Phys. A **505**, 215 (1989).
19. S.N. Ershov *et al.*, Phys. Rev. C **70**, 054608 (2004).
20. D.R. Tilley *et al.*, Nucl. Phys. A **708**, 3 (2002).